Gas-Phase Hydrogen/Deuterium Exchange of 5′- and 3′-Mononucleotides in a Quadrupole Ion Trap: Exploring the Role of Conformation and System Energy

Joseph E. Chipuk and Jennifer S. Brodbelt
Department of Chemistry and Biochemistry, University of Texas at Austin, Austin, Texas, USA

Gas-phase hydrogen/deuterium (H/D) exchange reactions for deprotonated 2′-deoxy-5′-monophosphate and 2′-deoxy-3′-monophosphate nucleotides with D_2O were performed in a quadrupole ion trap mass spectrometer. To augment these experiments, molecular modeling was also conducted to identify likely deprotonation sites and potential gas-phase conformations of the anions. A majority of the 5′-monophosphates exchanged extensively with several of the compounds completely incorporating deuterium in place of their labile hydrogen atoms. In contrast, most of the 3′-monophosphate isomers exchanged relatively few hydrogen atoms, even though the rate of the first two exchanges was greater than observed for the 5′-monophosphates. Mononucleotides that failed to incorporate more than two deuterium atoms under default reaction conditions were often found to exchange more extensively when reactions were performed under higher energy conditions. Integration of the experimental and theoretical results supports the use of a relay exchange mechanism and suggests that the exchange behavior depends highly on the identity and orientation of the nucleobase and the position and flexibility of the deprotonated phosphate moiety. These observations also highlight the importance of the distance between the various participating groups in addition to their gas-phase acidity and basicity. (J Am Soc Mass Spectrom 2007, 18, 724–736) © 2007 American Society for Mass Spectrometry

Hydrogen/deuterium (H/D) exchange has become a valuable tool for obtaining conformational information about gas-phase molecules [1–30]. In recent years considerable effort has been invested to understand the mechanisms of gas-phase H/D exchange. Rigorous molecular modeling has often been used to clarify the locations of the exchanged sites or the kinetics of exchange based on accessibility of labile hydrogens and the ability of key functional groups to interact. Such studies are increasingly aimed at elucidating the conformations of biological molecules in the gas phase, ones for which secondary structures are complex and critical for function in solution.

Gas-phase H/D exchange reactions involve the formation of an ion-molecule complex [14, 15]. The lifetime of this complex is important, as results from numerous experiments have demonstrated that the exchange rate depends on the difference in the gas-phase acidity or basicity of the analyte and the deuterating reagent [14, 15, 31], as well as the conformational access of the deprotonation site and deuterating agent to various reactive hydrogen atoms [15, 20, 21]. It is therefore not surprising that the bulk of the gas-phase H/D exchange studies have been performed using either a quadrupole ion trap (QIT) [1–13] or, more predominantly, a Fourier transform ion-cyclotron resonance (FTICR) mass spectrometer [14–27], since these two techniques are well suited to trapping ions for variable periods to allow kinetic analysis. While the two methodologies have many fundamental similarities, they also have several inherent differences that impact the results of ion-molecule reaction experiments, including the temperatures of ions, the number of collisions that they undergo with the reagent or buffer gas, and the total reaction time.

Deoxyribose monophosphate nucleotides (Figure 1) are the fundamental building blocks of oligonucleotides and engage in an array of intermolecular hydrogen bonds that are important for building the complicated secondary structure of DNA. FTICR mass spectrometry has been used to study gas-phase H/D exchange of both anionic [18, 19, 21] and cationic [22] mononucleotides. Robinson et al. studied both 5′- and 3′- mononucleotides using D_2O as a deuterating agent and showed that in some cases the extents and rates of exchange varied with both the nucleobase and position of the terminal phosphate group [18]. In addition, key

Published online February 6, 2007

Address reprint requests to Dr. Jennifer S. Brodbelt, Department of Chemistry and Biochemistry, 1 University Station A5300, University of Texas at Austin, Austin, TX 78712. E-mail: jbrodbelt@mail.utexas.edu

© 2007 American Society for Mass Spectrometry. Published by Elsevier Inc.
1044-0305/07/$32.00
doi:10.1016/j.jasms.2006.12.007

Received December 10, 2006
Revised December 18, 2006
Accepted December 19, 2006

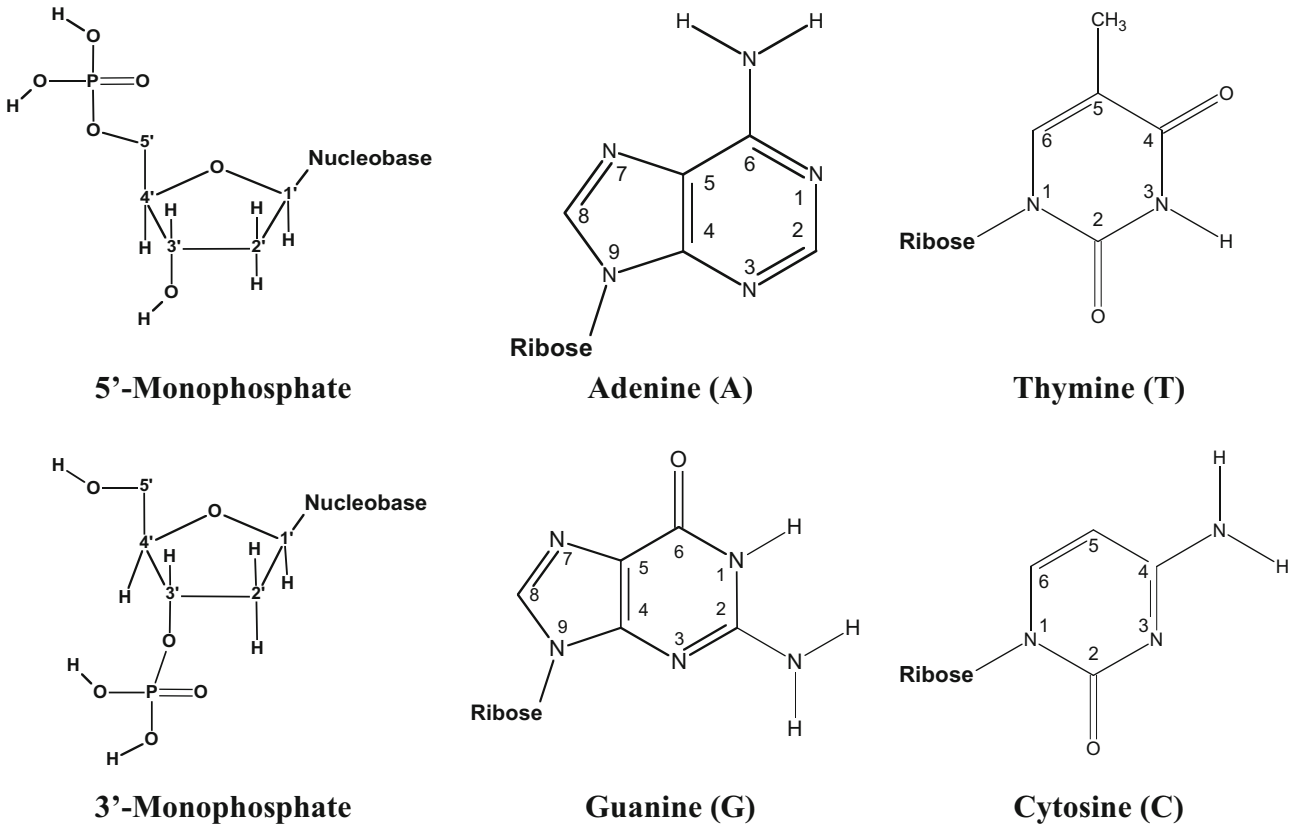

Figure 1. Canonical structures of the 2′-deoxy monophosphate nucleotides. The phosphate group can be located at either the 3′- or 5′-position of the ribose. As indicated, each monophosphate structure also contains one of the nucleobases attached via the N-glycosidic bond at either the N9 or N1 position.

results for the 3′, 5′-cyclic monophosphate nucleotides suggested that the most probable mechanism of exchange required both spatial proximity and cooperation between the phosphate group and the nucleobase; a result consistent with a relay mechanism first proposed using protonated amino acids [14] and glycine oligomers [15], and subsequently confirmed by a detailed examination of 5′- adenosine monophosphates [21]. As shown in Scheme **1**, the relay mechanism requires the formation of a hydrogen-bonded complex between a hydrogen donor site of the target compound, the deuterating reagent, and a deuterium acceptor site of the target compound, in which the deuterating reagent must bridge two sites of the target compound, thus restricting the maximum distance spanned between the hydrogen donor and acceptor sites [7, 32].

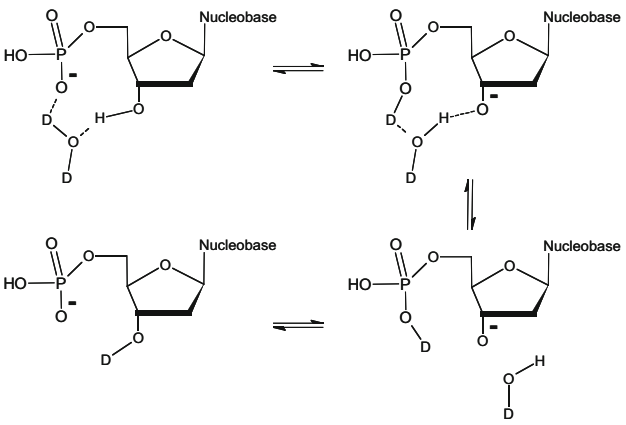

Scheme 1. H/D exchange via the relay mechanism.

The H/D exchange of mononucleotides using D_2O in the FTICR produced relatively few exchanges [18, 19]. Therefore, alternate deuterating agents were investigated, and it was shown that the use of D_2S as a deuterating agent significantly enhanced the rates and often the extents of these reactions [19]. However, regardless of the deuterating agent used, none of the H/D exchange reactions of the 5′-monophosphate nucleotides were observed to go to completion, even at reaction times up to 360 s [18, 19].

In addition to the H/D exchange experiments described above, extensive theoretical modeling and ion mobility (IM) studies have been performed on the deprotonated 5′-mononucleotides [33]. Although the computational results suggested the existence of two families of low-energy conformations, only one peak was observed in the IM arrival time distributions at temperatures as low as 80 K. These results implied that either only one family of conformers existed for the

deprotonated mononucleotides or that if multiple conformations did exist, the energy barriers to interconversion were relatively low and anions could sample rapidly the different structures during their time in the drift cell.

The present work focuses on the examination of the gas-phase H/D exchange behavior of both anionic 3′- and 5′-mononucleotides in a quadrupole ion trap. Since the results of the H/D exchange reactions are likely to be different than those obtained by FTICR mass spectrometry, the experiments performed here serve as a basis for future work involving gas-phase studies of more complex oligonucleotides in a quadrupole ion trap mass spectrometer. Thus, the observed trends will be critical for the successful interpretation of future results.

Experimental

Chemical Reagents

Monophosphate 2′-deoxynucleotides [e.g., 2′-deoxyadenosine-5′-monophosphate (5′-dAMP), 2′-deoxycytidine-5′-monophosphate (5′-dCMP), 2′-deoxyguanosine-5′-monophosphate (5′-dGMP), 2′-deoxythymidine-5′-monophosphate (5′-dTMP), 2′-deoxyadenosine-3′-monophosphate (3′-dAMP), 2′-deoxycytidine-3′-monophosphate (3′-dCMP), 2′-deoxyguanosine-3′-monophosphate (3′-dGMP), and 2′-deoxythymidine-3′-monophosphate (3′-dTMP)] were purchased from Sigma-Genosys (The Woodlands, TX) as desalted standards. D_2O was purchased from Sigma-Aldrich (St. Louis, MO). All of these compounds were used without further purification. Stock standards of the mononucleotides (10^{-3} M) were prepared in water. Working standards (4.0×10^{-5} M) were prepared by diluting a fraction of the appropriate stock standard with the requisite amount of HPLC grade methanol.

ESI-QIT Mass Spectrometry

The instrument used for the analyses was a Hitachi (Japan) 3DQ quadrupole ion trap mass spectrometer (model: M-8000 LC/3DQMS) equipped with an electrospray ionization (ESI) source. The nitrogen sheath gas of the ESI source was set to 2.2 kg/cm^2 and the helium buffer gas inside the trap was set to 3.0 kg/cm^2, yielding a helium pressure of ~1 mTorr. Mononucleotide solutions (4.0×10^{-5} M) flowing from a syringe pump at 15 μL/min were combined with a makeup flow of 120 uL/min HPLC grade methanol to provide a total flow of 135 μL/min to the ESI source. This procedure is an artifact of the 3DQ source which is designed for HPLC applications, thus reducing the effective concentration to 5.6×10^{-6} M. The adjustable temperature settings of the electrospray source were set as follows: assist gas heater 200° C, desolvator 200° C and aperture 1 190° C. The ESI probe, drift and focus voltages were optimized as necessary with typical values being 2.8 kV, 65V, and 40 V, respectively. All analyses were performed in the negative ion mode with the photomultiplier detector voltage set at 610 V.

Several temperature-variable H/D exchange reactions were also undertaken for selected deprotonated 2′-deoxy-mononucleotides to investigate the impact of increasing the energy of the ions on the observed extent of exchange. The internal temperature of the quadrupole ion trap was monitored by attaching an external thermocouple (K series) to the feedback leads running to the instrument control board. Under default conditions the Hitachi ion trap is heated resistively at a constant 5 V and has a measured equilibrium trap temperature near 55° C. Attachment of a variable voltage source (0 to 15 V) to the resistive heater allowed the trap to be heated to temperatures greater than 55° C, with a maximum near 125° C. While these higher temperatures are not necessarily optimal for spectrometric performance of the quadrupole ion trap, they do allow the temperature of the trap to be used as an additional experimental variable. The instrument was also equipped for direct laser irradiation of the internal volume of the ion trap by focusing a Synrad CO_2 laser through a zinc selenide window. In the experiments that involved laser irradiation, the laser power was held at a very low percent (usually ≤5%) of 50 W maximum to avoid analyte fragmentation.

H/D Exchange

All of the H/D exchange reactions were conducted in the gas phase inside the quadrupole ion trap. Deuterium oxide (D_2O) was used as the deuterating agent and introduced to the ion trap via a custom leak valve assembly° as° described° previously° [10].° Using° this arrangement, the exchange gas was admitted to the ion trap independent of the helium buffer gas. The typical base pressure of the system including helium buffer gas was nominally 5×10^{-5} torr as measured by the ion gauge. The extent of exchange was observed by monitoring the relative abundance of the precursor ion and deuterated species while the pressure of the exchange reagent was held near 3.5×10^{-4} torr. Ions were accumulated for 25 ms with a subsequent isolation time of 10 ms. Reaction times with D_2O varied over several orders of magnitude with the maximum time being 10 s. Each mononucleotide was analyzed individually and followed immediately by a similar series of experiments for the complementary isomer. In addition, experiments were repeated on at least one other day under very similar if not identical conditions to assess reproducibility.

The KINFIT program is a downloadable Microsoft excel add-in that is used for data fitting by solving sets of°coupled°ordinary°differential°equations°[34].°Here°it was used to estimate rate constants and construct kinetic plots for the H/D exchange reactions using the default parameters for H/D exchange located in the program code. Before data fitting, all data were normalized and isotopic corrections to peak intensities were

made based on the theoretical amounts of ^{13}C in each peak. Peaks that were less than 1% of the intensity of the base peak were omitted from the equation fitting. In addition, exchange factors were calculated at 100 ms by taking the sum of the peak heights for all deuterium-exchanged ions divided by the sum of the height of the unexchanged precursor and the calculated abundance of its ^{13}C isotope [6].

Molecular Modeling

All molecular modeling was performed in house using the CAChe Worksystem Pro package and Gaussian 03W [35]. Ab initio determination of the gas-phase acidities of the various deprotonation sites of the mononucleotides was performed using a multi-step process. The CAChe program was used to perform an initial optimization of the geometry of each mononucleotide by first utilizing the MM3 [36] force field and then conducting a subsequent optimization at a semi-empirical level of theory using the AM1 [37] parameterization. The optimized Cartesian atomic coordinates from the AM1 procedure were used as the input for a final ab initio optimization of the geometry using the restricted Hartree-Fock (RHF) level of theory and the 6-31G(d) basis set in Gaussian. This model chemistry is prominent through much of the literature and has been shown to be quite adequate for predicting molecular geometry [38]. Frequency calculations were also performed with RHF/6-31G(d) to both insure that the optimized geometries were a local minimum and to obtain a value for the zero point energy correction (ZPE). Zero point energies were scaled appropriately using the factor of 0.9135 as reported by Pople et al. [39]. Final single point energies (SPE) of the mononucleotides were calculated using the RHF optimized nuclear coordinates and the B3LYP/6-311++G(d,p) model chemistry.

Calculation of the relative acidities of each potential deprotonation site was completed to assess the most likely location of the negative charge. The gas-phase acidity corresponds to the energy difference between a neutral molecule and its deprotonated form, with the labile proton having the greatest gas-phase acidity being the most likely one lost in the ionization process. With the total energy of a species being approximately the sum of its single point energy and corrected zero point energy, the acidity can be calculated as $\Delta H_{acidity} = \Delta H_{HA-} \Delta H_{A-}$ where $\Delta H_{HA} = SPE_{HA}\text{-}ZPE^{corr}{}_{HA}$ for the neutral molecule and $\Delta H_{A-} = SPE_{A-} - ZPE^{corr}{}_{A-}$ for the anion.

In addition to the acidity calculations, dynamic simulations were carried out to investigate possible low-energy gas-phase conformations and to evaluate the impact of variations in conformation on the distance between the deprotonated charge site and the remaining exchangeable hydrogens. In each case the optimized RHF/6-31G(d) geometry from the acidity calculation was used as a starting point for a simulated annealing approach similar to that described previously [33]. In the annealing procedure an optimized starting structure was heated for 30 ps at 800 K then subjected to a second cooling of 10 ps at 0 K using the augmented MM3 force field and energy minimized again. The resulting structure was saved and used as the starting structure for a subsequent annealing cycle. A total of 100 annealing cycles were completed and the resulting conformations were sorted by potential energy. The lowest energy conformation(s) were then subjected to additional molecular dynamics simulations of 1000 ps at 300 K. In these simulations, snapshots were saved every 1 ps to generate a total of 1000 conformations per simulation that tracked the molecular motion over time. Distances between key atoms were then calculated using the Cartesian coordinates of the nuclear centers for each snapshot.

Results and Discussion

Gas-Phase Acidity Calculations

Intuitively, the phosphate group is expected to be the most acidic functional group of the mononucleotides. Prior gas-phase acidity calculations using isolated nucleobases and carefully chosen model compounds supported this hypothesis [18, 19, 21]. However, those calculations were not capable of capturing any of the potential intramolecular interactions between the phosphate group, the hydroxyl group of the ribose, and nucleobase that could stabilize many of the mononucleotide structures. Since these types of intramolecular interactions could differ for the two isomeric groups studied here, it was deemed prudent to calculate the gas-phase acidities of the complete monophosphate nucleotides.

Several conclusions can be drawn from the acidity results presented in Table 1. Foremost are the affirmations that the phosphate group is the most likely site of deprotonation for the 5′-monophosphate nucleotides and that the nucleobases are not favorable deprotonation sites for either set of isomers. These results indicate that any exchange involving these labile nucleobase hydrogens via a relay mechanism must depend on the relative location of the other possible deprotonation sites.

The calculated acidities for the 3′-phosphate groups and 5′-hydroxyl groups of the 3′-monophosphate nucleotides were found to be very similar due to the formation of a hydrogen bond between the phosphate group and ribose hydroxyl group when the charge was placed at either of the two sites. Interestingly, this hydrogen bond was not apparent when the 5′-monophosphates were deprotonated at the 3′- ribose hydroxyl group. Therefore, while deprotonation of the phosphate group confirmed the same hydrogen-bonded conformation as identified by both Amber molecular mechanics [33, 40] and semi-empirical calculations [18], charge localization at the 3′-ribose position did not. These calculations suggest that an energy barrier may impede the for-

Table 1. Gas-phase acidities of 5′- and 3′-phosphate mononucleotides[a]

Mononucleotide	Deprotonation Site	Acidity (kcal/mole)	Acidity Difference[b] (kcal/mole)
5′-dAMP	Phosphate	322.8	0.0
	Ribose Hydroxyl	342.2	19.4
	Base Nitrogen	351.6	28.8
5′-dCMP	Phosphate	320.2	0.0
	Ribose Hydroxyl	348.3	28.1
	Base Nitrogen	348.9	28.7
5′-dGMP[c]	Phosphate	305.4	0.0
	Ribose Hydroxyl	339.3	33.9
	Base Nitrogen-1	321.0	15.6
	Base Nitrogen-2	322.8	17.4
5′-dTMP	Phosphate	302.9	0.0
	Ribose Hydroxyl	308.4	5.6
	Base Nitrogen	334.0	31.1
3′-dAMP	Phosphate	310.2	0.0
	Ribose Hydroxyl	310.5	0.3
	Base Nitrogen	349.8	39.6
3′-dCMP	Phosphate	308.1	0.0
	Ribose Hydroxyl	308.2	0.1
	Base Nitrogen	339.7	31.6
3′-dGMP[c]	Phosphate	308.0	0.0
	Ribose Hydroxyl	309.3	1.3
	Base Nitrogen-1	327.7	19.7
	Base Nitrogen-2	329.5	21.5
3′-dTMP	Phosphate	307.3	0.0
	Ribose Hydroxyl	310.0	2.7
	Base Nitrogen	341.9	34.6

[a]Calculated at the B3LYP/6-311++G(d,p)//RHF/6 31G(d) level of theory.
[b]Tabulated acidity difference is the difference between the given deprotonation site and the most acidic site for that molecule.
[c]For the guanosine isomers the labile hydrogen on the secondary amine is labeled Base Nitrogen-1, while the labile hydrogens on the primary amine are labeled as Base Nitrogen-2.

mation of the hydrogen-bonded conformation when the charge is remote from the 5′-phosphate group. The height of this barrier is unknown, but it may influence the relative behaviors of the 5′- and 3′-monophosphate nucleotides if the negative charge were to become localized at the ribose following H/D exchange via the relay mechanism.

H/D Exchange

The typical progression of the hydrogen/deuterium exchange reactions of the 2′-deoxy mononucleotide anions with D_2O inside the quadrupole ion trap (QIT) is exemplified by the reaction of 2′-deoxy-5′-cytidine monophosphate (5′-dCMP) shown in Figure 2. As the reaction time increased from 10 ms to 10 s, an increase in the abundance of the deuterated ions D(1), D(2), D(3), and D(4) was observed with a corresponding decrease in the abundance of the precursor ion, D(0). The kinetic data that were gathered for this exchange reaction are depicted in Figure 3. Similar kinetic plots were used to calculate the rate constants for the reactions of each deprotonated 2′-deoxy-monophosphate nucleotide with D_2O. Both the exchange factors at 100 ms and the rate constants are summarized in Table 2.

In some cases, as observed for 5′-dCMP in Figures 2 and 3, the reaction resulted in complete exchange of all the labile hydrogens for deuterium. In other cases exchange ceased after the complete exchange of only several of the available hydrogens and continued reaction time produced no further exchange. After a reaction time of 10 s, all of the deprotonated 2′-deoxy-mononucleotides, including both 5′- and 3′-phosphate compounds, were observed to exchange at least two labile hydrogens. However, examination of the rate constants shows that in all cases the exchange of the first two protons occurred more quickly for the deprotonated 2′-deoxy-3′-phosphate mononucleotides than for the corresponding deprotonated 2′-deoxy-5′-phosphate mononucleotides. Furthermore, with the exception of 2′-deoxy-5′-adenosine monophosphate (5′-dAMP), exchange of all labile hydrogens was observed to some extent for all of the 5′-phosphate compounds. In contrast, 2′-deoxy-3′-guanosine monophosphate (3′-dGMP) was the only 3′-monophosphate isomer to exchange more than two labile protons. Thus, while the rate constants for D(1) and D(2) were larger for the 3′-monophosphate isomers, there were several cases where a greater extent of exchange was observed for the 5′-monophosphates despite having smaller rate constants for the first two exchanges.

Overall, the extent of exchange in the QIT was greater than or equal to that previously reported for

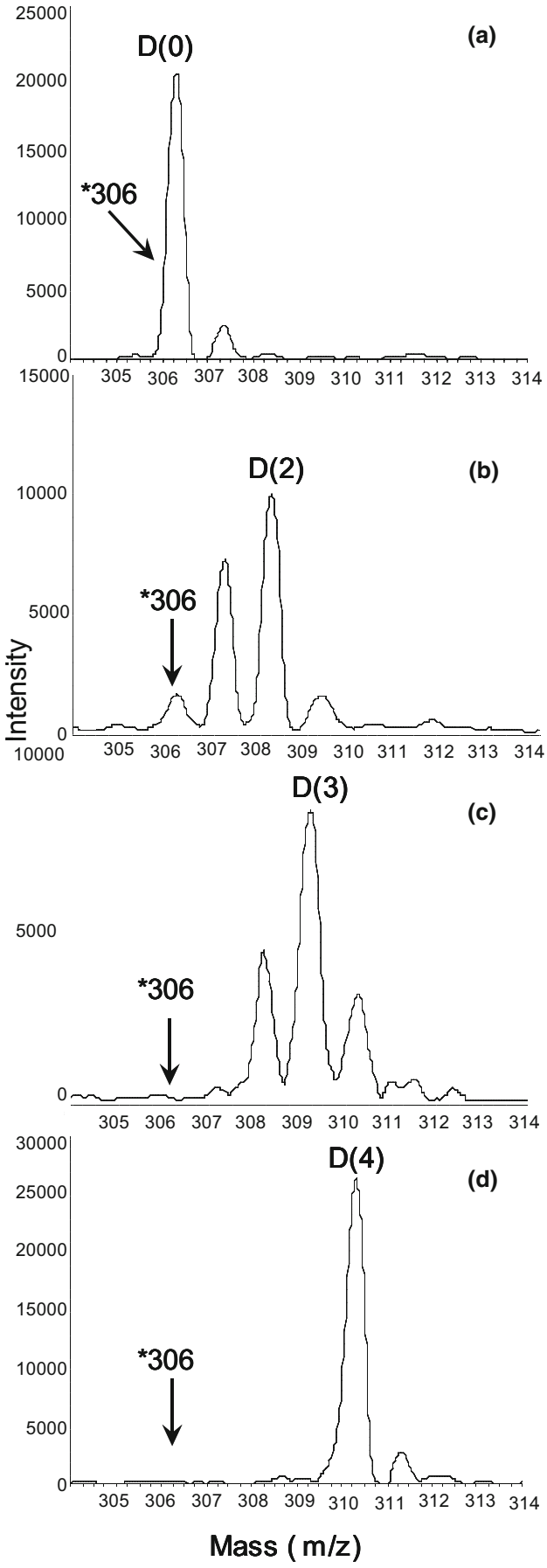

the FT-ICR instrument with several of the exchange reactions progressing to completion in the QIT, yet were reported by both Robinson et al. and Freitas et al. to terminate well short of completion in an FTICR mass spectrometer [18,19,21]. These differences are associated with the energy and gas-phase conformations of the ions as well as the number and frequency of ion-molecule collisions. The effective temperatures of ions in a quadrupole ion trap are thought to be higher than those in an FTICR mass spectrometer [41–42]. The gas-phase conformations of ions are temperature-dependent as demonstrated by numerous ion mobility studies [43] and, thus, there may be a greater range of gas-phase conformations of the mononucleotides in the quadrupole ion trap, as well as differences in the proximities and accessibilities of various labile hydrogens. Similar ion trap conditions to those utilized here have been previously reported to allow slightly higher energy conformations for pentapeptides and thus influenced their exchange reactivity [8]. In addition, the collision frequency and number are greater in the QIT than the FTICR and have been previously cited as being responsible for variations in the exchange behavior observed for peptide model compounds [14] and selected aspartic acid containing peptides [11].

2′-Deoxy-Cytidine and 2′-Deoxy-Thymidine Monophosphate Isomers (5′-dCMP, 3′-dCMP, 5′-dTMP, and 3′-dTMP)

For comparison, representative H/D exchange spectra for both deprotonated 5′-dCMP and 3′-dCMP after 10 s exchange time with D_2O in the QIT are shown in Figure 4a and b. For the 5′ phosphate isomer, the dominant product after 10 s incorporated four deuterium atoms, D(4), at *m/z* 310. The abundance of the ion of *m/z* 311 averaged 10.6% of the abundance of the ion of *m/z* 310 and was thus attributed primarily to the ^{13}C isotope of the D(4) product, not a true D(5) product. This spectrum shown in Figure 4a indicates that not only did 5′-dCMP reach the maximum number of exchangeable hydrogens (i.e., four) but also that the reaction proceeded to completion. The exchange behavior of deprotonated 3′-dCMP was quite different, with only two exchanges predominant after 10 s (Figure 4b). The D(2) product dominated as early as 2 s exchange time, and continued exposure to D_2O yielded no additional exchanges.

The H/D exchange reactions for both deprotonated 5′-dTMP and 3′-dTMP produced similar results to the

Figure 2. Representative mass spectra for the reaction of deprotonated 2′-deoxy-5′-cytidine monophosphate (5′-dCMP) with D_2O in a quadrupole ion trap. Reaction times are (**a**) 0 ms, (**b**) 250 ms, (**c**) 2000 ms, and (**d**) 10,000 ms.

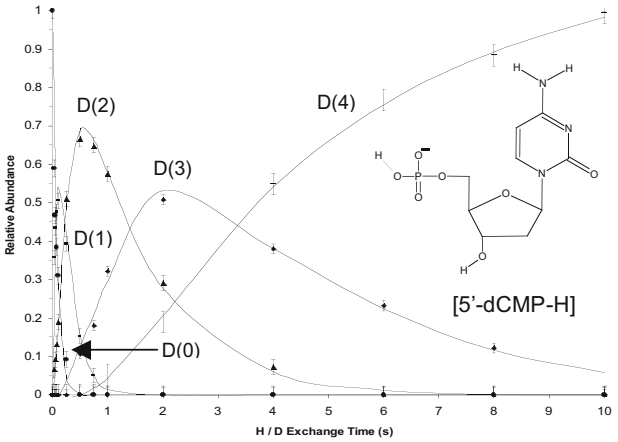

Figure 3. Kinetic plot of the H/D exchange reaction of deprotonated 2′-deoxycytidine-5′-monophosphate with D_2O using KINFIT [34]. D(0) represents the quickly disappearing unexchanged precursor ion, and D(1), D(2), D(3), and D(4) represent ions incorporating from one to four deuteriums. Error bars were calculated using the standard error of a series of replicate experiments taken over several days.

dCMP analogs. For the 5′- phosphate isomer, the dominant product after 10 s corresponded to the complete exchange of three deuterium atoms for hydrogen, D(3), with the reaction proceeding essentially to completion within 4 s. In contrast, the dominant product for deprotonated 3′-dTMP after as little as 500 ms and up to 10 s incorporated only two deuteriums, never three deuteriums as observed for the 5′-dTMP isomer.

These results can be rationalized by two factors associated with the structures of the mononucleotides (Figure 5a and b). When the phosphate is in the 5′-position, it is located on the same side of the ribose ring as the nucleobase, whereas the 3′-position places the two groups on opposing sides of the ring. The 5′-position is thus more favorable than the 3′-position for exchange of the nucleobase hydrogens via the relay mechanism because the distances between reactive sites are inherently greater when the groups are positioned opposite each other. Furthermore, when the phosphate is at the 5′-position, the four flexible bonds between the deprotonation site and the relatively rigid sugar provide an additional degree of freedom when compared with the 3′-phosphates, which have only three bonds between the charge site and the ribose. The additional flexibility facilitates an increase in the possible intramolecular interactions between the deprotonation site and more distant atoms. Therefore, the 5′-phosphate moiety may participate in several different exchange reactions for the cytidine and thymidine compounds, while the 3′-phosphate moiety is primarily stabilized by the interaction with the 5′-ribose hydroxyl group.

2′-Deoxy-Guanosine Monophosphate Isomers (5′-dGMP and 3′-dGMP)

For comparison, representative H/D exchange spectra for both deprotonated 5′-dGMP and 3′-dGMP after 10 s exchange time are shown in Figure 4c and d. For both isomers, the dominant product after 10 s incorporated four exchanges, D(4). Overall, the H/D exchange reactions of the 3′-dGMP isomer were much faster than that of 5′-dGMP, as illustrated by the greater rate constants in Table 2, and the exchange of four or five hydrogens was more complete than observed for the 5′-dGMP isomer. As evidenced by the steady growth in the product incorporating five deuteriums beyond 500 ms, possibly both dGMP isomers could eventually undergo complete exchange of all five labile hydrogens, resulting exclusively in the D(5) product, had the ion trap software allowed reaction times beyond 10 s.

As shown via REMPI spectroscopy [44] and in the modeling calculations performed in conjunction with this work and those performed previously [20, 33, 40], guanine was the only nucleobase to favor a −syn orientation that places it directly over the ribose ring in the gas phase (Figure 5c). For 5′-dGMP, this arrangement places the deprotonated phosphate group, the 3′-ribose hydroxyl and the nucleobase hydrogens in very close proximity. Stabilization can occur through forma-

Table 2. Relative apparent rate constants for H/D exchange of deprotonated mononucleotides reacting with D_2O

Mononucleotide[a]	Exchange factor at 100 ms[b]	k values[c]				
		k1	k2	k3	k4	k5
5′-dAMP (4)	∞	57.2	25.7	0.0	0.0	
5′-dCMP (4)	2.3	14.9	5.6	0.9	0.4	
5′-dGMP (5)	0.3	1.3	1.0	0.6	0.2	0.01
5′-dTMP (3)	0.7	5.6	3.3	1.2		
3′-dAMP (4)	∞	98.2	31.1	0.0	0.0	
3′-dCMP (4)	4.4	23.5	8.2	0.0	0.0	
3′-dGMP (5)	27.0	100.0	53.6	15.0	7.0	0.02
3′-dTMP (3)	2.7	15.8	7.4	0.0		

[a]The number of exchangeable hydrogens is shown in parentheses.
[b]Exchange factors (at 100 ms) were calculated as described in the literature [6] after isotopic corrections.
[c]Rate constant values as determined by kinetic fitting using Kinfit [34] after correcting for isotopic contribution and ignoring those corrected peaks that had a relative abundance of less than 5%. Rates reflect the number of exchanges per second, but the number of ions is unknown so the rates are relative and essentially unitless. All rate constants are reported relative to 3′-dGMP + D_2O and expressed as relative rate × 100.

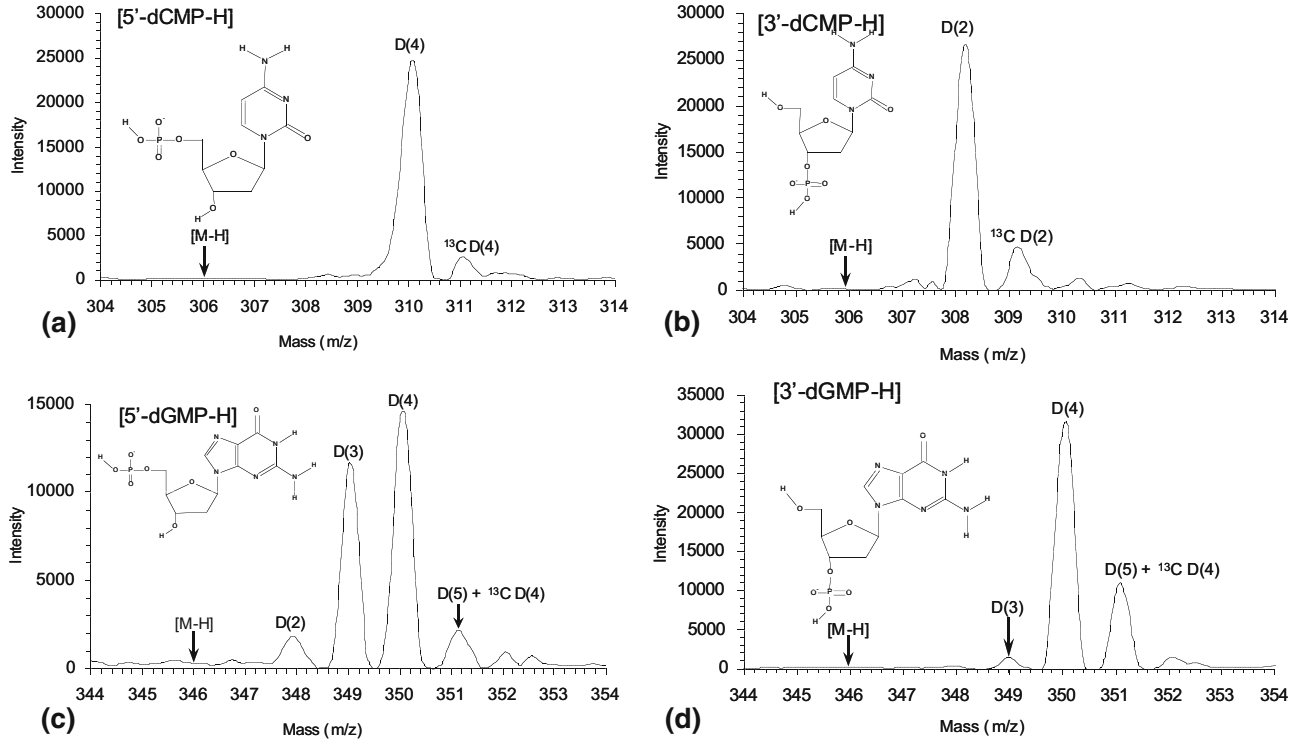

Figure 4. H/D exchange spectrum for (**a**) deprotonated 2′-deoxycytidine 5′-monophosphate (5′-dCMP), (**b**) deprotonated 2′-deoxycytidine 3′-monophosphate (3′-dCMP), (**c**) deprotonated 2′-deoxyguanosine 5′-monophosphate (5′-dGMP), and (**d**) deprotonated 2′-deoxyguanosine 3′-monophosphate (3′-dGMP) after 10 s exchange with D_2O.

tion of two hydrogen bonds involving the deprotonated phosphate, one with the ribose hydroxyl hydrogen and another with a primary amine hydrogen of the nucleobase. This conformation for 5′-dGMP might seem extremely suitable for a relay exchange mechanism as the deprotonation site is well within interacting distance of the labile hydrogen atoms. However, the stabilization of the labile hydrogens due to the hydrogen bonding actually appears to slow the reaction rate. This result coincides with other observations by Habibi-Goudarzi et al. for the dissociation of the mononucleotide anions by CID [45], Vrkic and O'Hair for the reaction with trimethylborate [13], and Yang et al. for the ionization energy [46], where the suspected intramolecular hydrogen bonding capability of 5′-dGMP was cited as the reason for the substantially different dissociation pattern, reactivity, and ionization energy, respectively.

Unlike the other 3′-phosphate mononucleotides, the −syn orientation of the guanine nucleobase enabled 3′-dGMP to exchange more than two hydrogens. However, in this case apparently the concerted intramolecular interactions among the phosphate, nucleobase and ribose hydroxyl group are not as strong as those in the 5′- isomer since very rapid exchange was observed for 3′-dGMP. These results echo what was reported by Robinson et al., where 3′-dGMP had not only the fastest exchange rate of the mononucleotides studied, but also was the only the 3′-phosphate to show appreciable exchange beyond D(2) [18]. Furthermore, it has recently been reported that the first water of hydration, a process that is analogous to complexation with D_2O, for the mononucleotides occurs at the phosphate group and may involve the deprotonated hydroxyl group and/or the doubly bonded oxygen atom [40]. Consequently, if the interaction between the deprotonated phosphate and primary amine hydrogen for 3′-dGMP is not as strong as that for 5′-dGMP, these hydrogens may be freed to interact more strongly with the first bound D_2O and their exchange could be responsible for the increased relative reaction rate. Therefore, while the proximities of the reactive sites may be important for exchange, these results also suggest that intramolecular hydrogen-bonding interactions that are too substantial may also limit the exchange rate. The important influence of hydrogen-bonding has also been discussed in the context of protein hydrogen exchange in solution [47]. Ultimately, there appears to be a critical distance and amount of interaction between reactive sites that optimizes the relay exchange mechanism in the gas phase.

2′-Deoxy-Adenosine Monophosphate Isomers (5′-dAMP and 3′-dAMP)

Unlike the other purine nucleotides, (5′-dGMP and 3′-dGMP), neither deprotonated 5′-dAMP or 3′-dAMP exchanged more than two deuteriums atoms. While the rates of exchange of the first two protons were among the fastest of all the mononucleotides, as indicated by

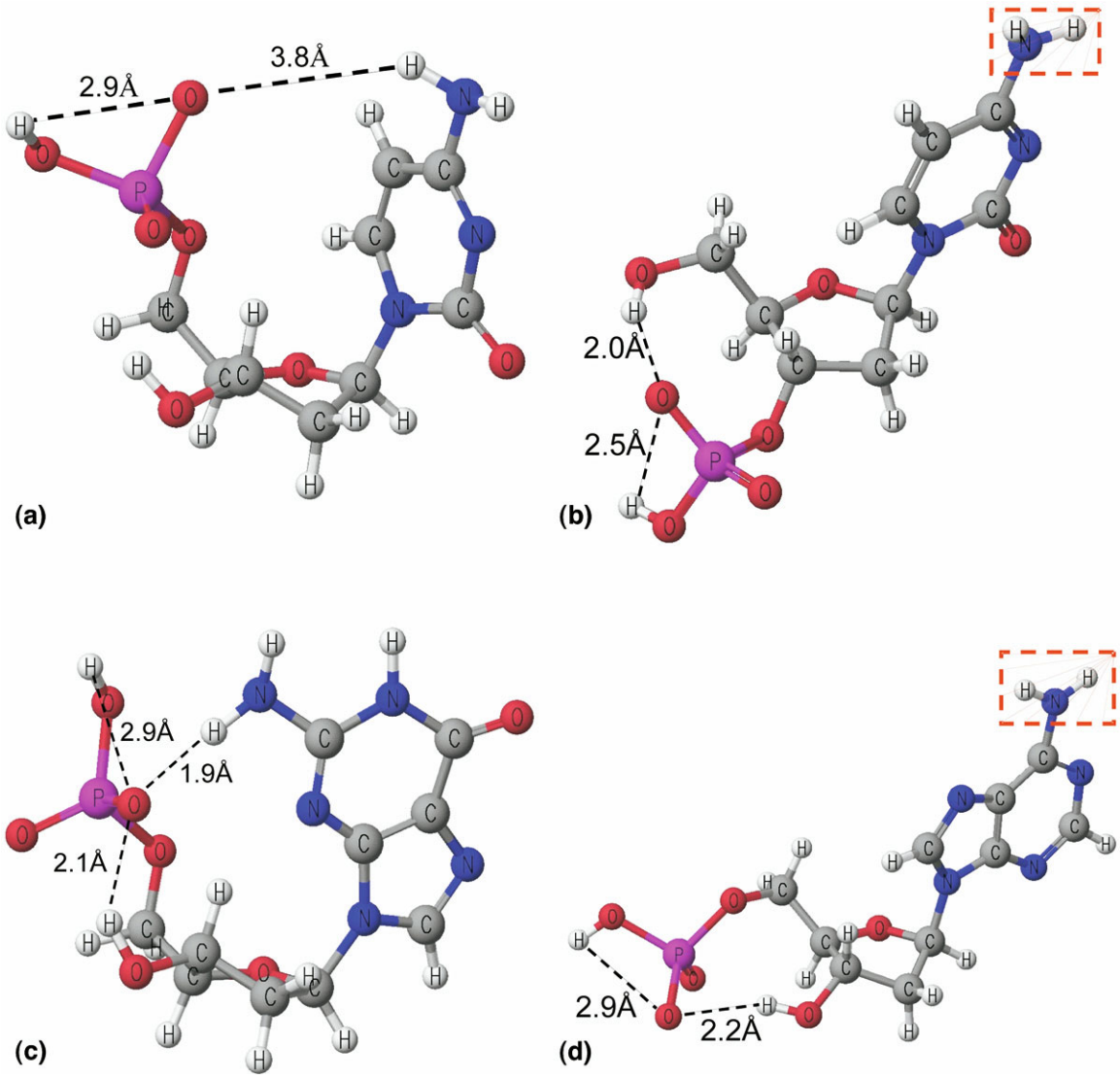

Figure 5. Molecular dynamics conformation of (**a**) deprotonated (phosphate) 5′-dCMP, (**b**) deprotonated (phosphate) 3′-dCMP, (**c**) deprotonated (phosphate) 5′-dGMP and d) deprotonated (phosphate) 5′-dAMP. Annotated distances indicate likely participants in H/D exchange via the relay mechanism. Dashed boxes demonstrate the relative seclusion of nucleobase hydrogens from the deprotonated phosphate for 3′-dCMP and 5′-dAMP.

the large relative rate constants shown in Table 2, the reaction effectively ceased after as little as 250 ms and longer reaction times up to 10 s, failed to produced additional exchange.

In contrast to the guanidine nucleobase that has labile hydrogens at the 2 position, the canonical form of the adenine has a primary amine at the 6 position, which tends to orient itself away from the deprotonated site when the nucleobase is rotated about the N-glycosidic bond. Without the stabilizing interaction of a hydrogen bond between the nucleobase and the deprotonated phosphate, the adenine mononucleotides will tend to favor an anti nucleobase orientation (Figure 5d). In this orientation, the increased size of the purine ring compared with the pyrimidine ring places the labile hydrogens too distant from the deprotonation site to engage in the relay mechanism. Therefore, the H/D exchange behavior of the adenine mononucleotide isomers primarily involves the interaction of the deprotonated phosphate and the ribose hydroxyl group. Since these groups interact readily in both 5′- and 3′-phosphates, the H/D exchange behavior of the two adenosine isomers should be independent of the phosphate position, as is evident by the nearly identical exchange behavior observed in the present study.

Molecular Dynamics Simulations

Molecular dynamics simulations were performed to probe the various gas-phase conformations of the deprotonated mononucleotides. The previous molecular dynamics simulations performed on the 5′-phosphate mono-

nucleotides identified two conformational families with the key variations attributed to the twist in the sugar ring and the relative orientation of the nucleobase [33]. The dominant family of conformations was reported to have the deprotonated phosphate hydrogen-bonded to the 3′-hydroxyl group and the nucleobases above the ring with the sugar in a C3′-endo position [33]. These calculations suggested that the adenine, cytosine, and thymine bases tended to orient themselves in an anti-position, whereas the guanidine base preferred a syn-position. Modeling investigations of cyclic mononucleotides cGMP [48] and cAMP [49], compounds similar to a mononucleotide that has the deprotonated phosphate and ribose hydroxyl group hydrogen-bonded, also suggest these nucleobase orientations. Here, calculations analogous to those performed by Gidden et al. [33] have been performed not only on the 5′-phosphates, but also extended to the 3′-phosphate mononucleotide isomers. Instead of examining collision cross section, as was done for the previous study, the focus here was on the distances between the deprotonated phosphate and the other groups of labile hydrogens as a means to investigate the feasibility of hydrogen/deuterium exchange via the relay mechanism.

For all of the dynamics simulations, the negative charge was assigned to one of the deprotonated oxygen atoms attached to the phosphorus atom. In reality, this charge is delocalized over the entire phosphate moiety, and the remaining labile hydrogen likely shuttles between the two possible deprotonation sites of the phosphate group. Not surprisingly, this hydrogen atom was consistently calculated to be less than 4 Å away from the assigned charge site. In addition, simulation results for both the 2′-deoxy-5′-monophosphate nucleotides and the 2′-deoxy-3′-monophosphate nucleotides indicated that the ribose OH group and the phosphate also tended to be in close proximity (i.e., a distance of between 2 and 4 Å). These values did not vary greatly with the identity of the nucleobase for the 5′- or 3′-isomers, and thus the remaining phosphate hydrogen and ribose hydroxyl group should be expected to be highly probable exchange sites for all of the 5′- and 3′-mononucleotide ions.

In contrast, the distances between the phosphate ion and the labile hydrogen atoms on the nucleobases varied significantly across the series of mononucleotides and depended on both the identity of the nucleobase and the location of the deprotonated phosphate (5′- versus 3′- position). The mononucleotides with the shortest distance between the two moieties were the guanidine mononucleotides 5′-dGMP and 3′-dGMP due to the −syn orientation of the nucleobase (Figure 5c). The analogous distance calculations for the cytidine and thymidine isomers (5′-dCMP, 3′-dCMP, 5′-dTMP, and 3′-dTMP) produced relatively few conformations where the two reactive moieties were within 4 Å of each other and only a modest number where they were within 6 Å. In addition, the 5′-phosphate isomers of thymidine and cytidine tended to have many more accessible conformations than their 3′-phosphate counterparts. Finally, both the 5′- and 3′-adenine isomers produced almost no conformations where the phosphate/nucleobase distance was less than 6 Å, thereby making them the least likely of the nucleobases to exchange via the relay mechanism.

Overall, the results of the dynamics simulations correlate strongly to the experimental data. With deprotonation occurring at the phosphate, exchange of the remaining phosphate hydrogen and ribose hydroxyl hydrogen were identified as being readily accessible for exchange. Likely, these two hydrogen atoms compose the majority of the D(2) ions observed throughout the mononucleotide H/D exchange reactions. Furthermore, the relative proximity of the nucleobase to the phosphate appeared to correspond to the extent of exchange observed beyond D(2), as many accessible conformations were calculated for the mononucleotides observed to exchange extensively (5′-dGMP, 3′-dGMP, 5′-dCMP, and 5′-dTMP) while relatively few accessible conformations were identified for those compounds that exchanged only two hydrogens (5′-dAMP, 3′-dAMP, 3′-dCMP, and 3′-dTMP).

Temperature Variable H/D Exchange

In contrast to the H/D exchange observed for the other deprotonated mononucleotides, the reactions involving 5′-dAMP, 3′-dAMP, 3′-dCMP, and 3′-dTMP incorporated a maximum of two deuterium atoms, D(2). In each case the precursor parent ion was completely converted to the D(2) ion within 2 s reaction time, and additional time failed to promote any further exchange. Molecular modeling results suggested that the two observed exchanges were likely to be associated with the remaining phosphate hydrogen and the ribose hydroxyl hydrogen, based on their calculated distances to the deprotonation site. In addition, it appeared that the labile nucleobase hydrogens of these four mononucleotides were isolated from the deprotonation site due to conformational restrictions and possible potential energy barriers. As described in the experimental section, additional resistive heating of the ion trap and direct laser irradiation of the ion packet were employed to increase the amount of energy available to the ions in an attempt to overcome these obstacles.

For three of the four aforementioned mononucleotides, the extent of H/D exchange after 10 s with supplemental ion trap heating increased beyond D(2) (results shown in Figure 6). The amount of increase varied however, with the results for 3′-dCMP showing the most dramatic change (Figure 6a and b). Significant proportions of both D(3) and D(4) ions were observed when the exchange reaction was conducted at an elevated trap temperature of 95° C, which is 40° C higher than the measured default trap temperature. Additional exchange was also observed for 3′-dTMP, although in this case the trap required significantly more heating (nominally 125° C) to produce an average of only 10% D(3) ions (spectra not shown).

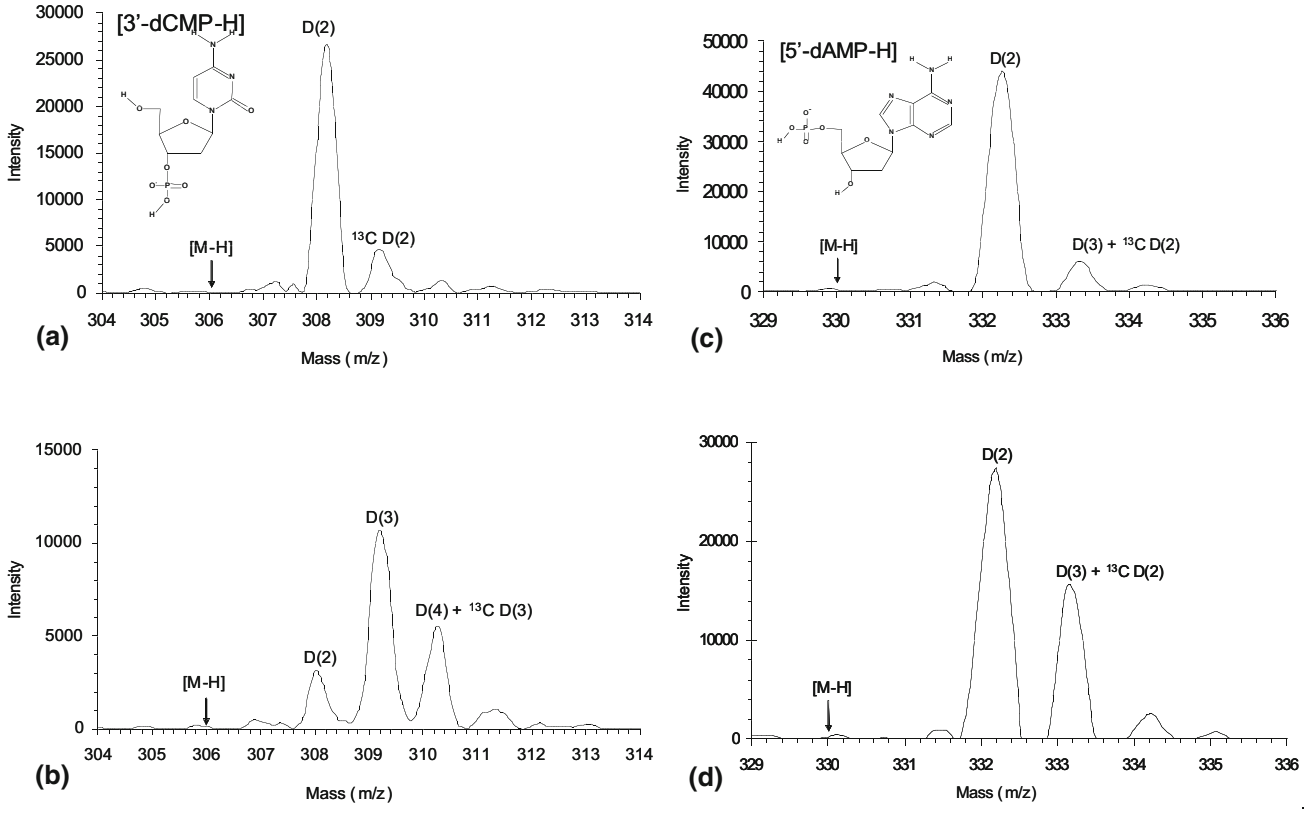

Figure 6. H/D exchange spectrum after ten seconds exchange with D_2O for (**a**) deprotonated 2′-deoxycytidine 3′-monophosphate (3′-dCMP) at the default ion trap temperature of 55° C, (**b**) deprotonated 2′-deoxycytidine 3′-monophosphate (3′-dCMP) at an elevated trap temperature of 95° C, (**c**) deprotonated 2′-deoxyadenosine 5′-monophosphate (5′-dAMP) at the default ion trap temperature of 55° C, and (**d**) deprotonated 2′-deoxyadenosine 5′-monophosphate (5′-dAMP) at an elevated trap temperature of 95° C with additional laser irradiation at 5% power.

The nucleobase labile hydrogens that were most resistant to exchange were those of the 2′-deoxyadenosine monophosphates, both 3′-dAMP and 5′-dAMP. With additional ion trap heating, (up to 125° C), neither of these compounds was observed to exchange beyond D(2), but instead showed cleavage of the nucleobase from the precursor ion. However, when 5′-dAMP was subjected to both direct laser irradiation and resistive heating of the ion trap to 95° C, the average abundance of the ion of *m/z* 332 (initially 11% due to the D(2)-^{13}C species) increased to over 47% compared with the abundance of the D(2) product of *m/z* 331 (Figure 6c and d). Additional heating or laser power in excess of 5% did not produce additional exchange, but again caused extensive fragmentation. Similar experiments were undertaken for deprotonated 3′-dAMP in which both the trap temperature and amount of direct laser irradiation were varied, however no additional exchange beyond D(2) was observed, regardless of the reaction conditions. Since heating alone was able to produce additional exchange for 3′-dCMP and 3′-dTMP, no laser irradiation experiments were conducted on these two mononucleotides.

The results in Figure 6, especially those for 3′-dCMP, demonstrate the considerable impact of the system energy on the observed H/D exchange spectra. While it would be convenient to infer that the additional exchanges are associated with the nucleobases, they could possibly involve hydrogens on carbon atoms. This type of energy-induced scrambling has been previously reported [23]. Another explanation is that the additional energy provided by the heating allows the ions to react via different exchange mechanisms, such as a more direct flip-flop mechanism that is independent of the relative positions of the deprotonated site and the labile hydrogen [15]. Furthermore, the additional energy may enable the mononucleotides to access different tautomeric forms in which a hydrogen atom shifts to an adjacent site accompanied by a migration of the adjacent double-bond that are more amenable to exchange. While it is not definitive, examination of the temperature variable results as a whole does provide some clarification.

First, while an increase in exchange was observed for 3′-dTMP, it required much more heat (70° C above default) than for 3′-dCMP and was very modest, resulting in only 10% of the D(3) ion. Moreover, exchange of 5′-dAMP could not be enhanced by heating alone and

required additional energy in the form of laser irradiation, and no increase in the extent of exchange could ever be induced for 3′-dAMP. Thus, apparently additional exchange is dependant on the identity of the nucleobase, thereby disfavoring the explanation of scrambling at the ribose ring.

Second, closer examination of the nucleobases reveals that the canonical forms of cytosine and adenine contain similar secondary amine groups that would be expected to form identical six-membered ring complexes with D_2O if a flip-flop mechanism were employed. Thus, the increase in exchange for 3′-dCMP, but lack of additional exchange for 3′-dAMP, suggests that a flip-flop mechanism is not involved. The lack of additional exchange for 3′-dAMP versus 5′-dAMP also weighs against the contribution of a flip-flop mechanism because the phosphate group apparently continues to play a role in the exchange.

Finally, one must consider the contribution of tautomeric forms of the nucleobases [50–53]. In most cases, both experimental and computational results suggest that the biologically relevant canonical forms are predominant at room temperatures [53]. However, energy barriers between tautomeric forms vary with the nucleobases as cytosine and guanine both have gas-phase tautomers that are reported to be within a few kcal/mol of the global minimum [50, 53]. The corresponding results for thymine and adenine suggested that their biologically relevant tautomeric forms were substantially higher in energy [50–52]. The most accessible forms were reportedly between 11 and 18 kcal/mol greater in energy, while other rare forms were disfavored by more than 30 kcal/mol. Therefore, there is evidence to support the existence of tautomers of cytosine in the gas phase, especially at increased temperatures. Depending on the amount of energy available, it may also be possible to find tautomers of thymine or adenine, but significant energy barriers would need to be overcome. Thus, tautomerization could contribute to the observed deviations in exchange behavior for 3′-dCMP and possibly 3′-dTMP and 5′-dAMP at higher temperatures. While the exact mechanism for the additional H/D exchange remains unclear, evidence does support that it is both dependent on the nucleobase, either in its canonical or tautomeric form, and the relative location of the phosphate moiety.

Conclusions

Studies have been performed on both the 5′- and 3′-monophosphate nucleotides to assess their ability to exchange with a common deuterating agent, D_2O, in a quadrupole ion trap. Variations in the exchange behaviors of the mononucleotide isomers confirm that the reactions are dependent on both the identity of the nucleobase and the position of the phosphate moiety. Several of the 5′-phosphate mononucleotides completely exchanged their labile hydrogen atoms while reactions involving the 3′-phosphate isomers terminated after exchange of only two deuteriums (i.e., dCMP and dTMP). In other cases, the exchange behavior between the isomers was similar, either because the nucleobase was not involved in the H/D exchange (i.e., dAMP) or because it was accessible to the deprotonated phosphate in either of the ribose positions (i.e., dGMP). The distinction between mononucleotide isomers by H/D exchange pattern shows promise for distinguishing sequences of larger oligonucleotides.

Extensive molecular modeling confirmed that the phosphate was the most likely deprotonation site of the mononucleotides and calculated distances between the phosphate and various labile hydrogens of conformations generated from molecular dynamics correlated strongly with experimental H/D exchange results. Mononucleotides with gas-phase conformations that kept the labile nucleobase hydrogens remote from the phosphate most likely exchanged only their phosphate and ribose hydroxyl hydrogen atoms. Again, these results were dependent on the flexibility of the phosphate and the orientation of the nucleobase.

Further experimentation using elevated trap temperatures and direct laser irradiation demonstrated that it is often possible to increase the extent of H/D exchange. These results suggest that the energy of the ions is vital to the observed exchange behavior and that increasing this energy has an impact on accessibility of gas-phase conformations of the canonical and possibly tautomeric forms of the ions. These results emphasize the importance of the reaction conditions in H/D exchange experiments and suggest the potential utility of conducting exchange reactions of larger oligonucleotides under a range of energy conditions.

Acknowledgments

The authors gratefully acknowledge funding from the Robert A. Welch Foundation (F-1155) and the National Institutes of Health (RO1 GM65956).

References

1. Kaltashov, I. A.; Doroshenko, V. M.; Cotter, R. J. Gas Phase Hydrogen/Deuterium Exchange Reactions of Peptide Ions in a Quadrupole Ion Trap Mass Spectrometer. *Proteins: Struct. Funct. Genet.* **1997**, *28*, 53–58.
2. Reid, G. E.; O'Hair, R. A. J.; Styles, M. L.; McFadyen, W. D.; Simpson, R. J. Gas Phase Ion-Molecule Reactions in a Modified Ion Trap: H/D Exchange of Noncovalent Complexes and Coordinatively Unsaturated Platinum Complexes. *Rapid Commun. Mass Spectrom.* **1998**, *12*, 1701–1708.
3. Reid, G. E.; Simpson, R. J.; O'Hair, R. A. J. Probing the Fragmentation Reactions of Protonated Glycine Oligomers Via Multistage Mass Spectrometry and Gas-Phase Ion-Molecule Hydrogen/Deuterium Exchange. *Int. J. Mass Spectrom.* **1999**, *191*, 209–230.
4. Felix, T.; Reyzer, M.; Brodbelt, J. Hydrogen/Deuterium Exchange of Nucleoside Analogs in a Quadrupole Ion Trap Mass Spectrometer. *Int. J. Mass Spectrom.* **1999**, *191*, 161–170.
5. Hofstadler, S. A.; Sannes-Lowery, K. A.; Griffey, R. H. Enhanced Gas-Phase Hydrogen-Deuterium Exchange of Oligonucleotide and Protein Ions Stored in an External Multipole Reservoir. *J. Mass Spectrom.* **2000**, *35*, 62–70.
6. Reyzer, M. L.; Brodbelt, J. S. Gas-Phase H/D Exchange Reactions of Polyamine Complexes: $(M + H)^+$, $(M + \text{alkali metal}^+)$, and $(M + 2H)^{2+}$. *J. Am. Soc. Mass Spectrom.* **2000**, *11*, 711–721.
7. Schaaff, T. G. Stephenson, J. L., Jr.; McLuckey, S. A. Gas Phase H/D Exchange Kinetics: DI Versus D_2O. *J. Am. Soc. Mass Spectrom.* **2000**, *11*, 167–171.

8. Wyttenbach, T.; Paizs, B.; Barran, P.; Breci, L.; Liu, D.; Suhai, S.; Wysocki, V. H.; Bowers, M. T. The Effect of the Initial Water of Hydration on the Energetics, Structures, and H/D Exchange Mechanism of a Family of Pentapeptides: An Experimental and Theoretical Study. *J. Am. Chem. Soc.* **2003**, *125*, 13768–13775.
9. Mao, D.; Babu, K. R.; Chen, Y. L.; Douglas, D. J. Conformations of Gas-Phase Lysozyme Ions Produced from Two Different Solution Conformations. *Anal. Chem.* **2003**, *75*, 1325–1330.
10. Zhang, J.; Brodbelt, J. S. Gas-Phase Hydrogen/Deuterium Exchange and Conformations of Deprotonated Flavonoids and Gas-Phase Acidities of Flavonoids. *J. Am. Chem. Soc.* **2004**, *126*, 5906–5919.
11. Hermann, K.; Wysocki, V.; Vorpagel, E. R. Computational Investigation and Hydrogen/Deuterium Exchange of the Fixed Charge Derivative Tris(2,4,6-Trimethoxyphenyl) Phosphonium: Implications of the Aspartic Acid Cleavage Mechanism. *J. Am. Soc. Mass Spectrom.* **2005**, *16*, 1067–1080.
12. Hermann, K. A.; Kuppannan, K.; Wysocki, V. H. Fragmentation of Doubly-Protonated Ion Populations Labeled by H/D Exchange with CD_3OD. *Int. J. Mass Spectrom.* **2006**, *249-250* 93–105.
13. Vrkic, A. K.; O'Hair, R. A. J. Gas-Phase Reactions of Trimethylborate with the $[M - H]^-$ Ions of Nucleotides and Their Non-Covalent Homo- and Heterodimer Complexes. *Aust. J. Chem.* **2003**, *56*, 389–399.
14. Gard, E.; Grenn, M. K.; Bregar, J.; Lebrilla, C. B. Gas-Phase Hydrogen/Deuterium Exchange as a Molecular Probe for the Interaction of Methanol and Protonated Peptides. *J. Am. Soc. Mass Spectrom.* **1994**, *5*, 623–631.
15. Campbell, S. C.; Rodgers, M. T.; Marzluff, E. M.; Beauchamp, J. L. Deuterium Exchange Reactions as a Probe of Biomolecule Structure. Fundamental Studies of Gas Phase H/D Exchange Reactions of Protonated Glycine Oligomers with D_2O, CD_3OD, CD_3CO_2D, and ND_3. *J. Am. Chem. Soc.* **1995**, *117*, 12840–12854.
16. Wood, T. D.; Chorush, R. A.; Wampler, F. M., III; Little, D. P.; O'Conner, P. B.; McLafferty, F. W. Gas-Phase Folding and Unfolding of Cytochrome c Cations. *Proc. Natl. Acad. Sci. U.S.A.* **1995**, *92*, 2451–2454.
17. McLafferty, F. W.; Guan, Z.; Haupts, U.; Wood, T. D.; Kelleher, N. L. Gaseous Conformational Structures of Cytochrome *c*. *J. Am. Chem. Soc.* **1998**, *120*, 4732–4740.
18. Robinson, J. M; Greig, M. J.; Griffey, R. H.; Venkantraman, M.; Laude, D. A. Hydrogen/Deuterium Exchange of Nucleotides in the Gas Phase. *Anal. Chem.* **1998**, *70*, 3566–3571.
19. Freitas, M. A.; Shi, S. D.-H.; Hendrickson, C. L.; Marshall, A. G. Gas-Phase RNA and DNA Ions. 1. H/D Exchange of the $[M - H]^-$ Anions of Nucleoside 5′-Monophosphates (GMP, dGMP, AMP, dAMP, CMP, dCMP, UMP, dUMP), Ribose 5-Monophosphate, and 2-Deoxyribose 5-Monophosphate with D_2O and D_2S. *J. Am. Chem. Soc.* **1998**, *120*, 10187–10193.
20. Wyttenbach, T.; Bowers, M. T. Gas-Phase Conformations of Biological Molecules: The Hydrogen/Deuterium Exchange Mechanism. *J. Am. Soc. Mass Spectrom.* **1999**, *10*, 9–14.
21. Freitas, M. A.; Marshall, A. G. Gas-Phase RNA and DNA Ions. 2. Conformational Dependence of the Gas-Phase H/D Exchange of Nucleotide-5′-Monophosphates. *J. Am. Soc. Mass Spectrom.* **2001**, *12*, 780–785.
22. Green-Church, K. B.; Limbach, P. A.; Freitas, M. A.; Marshall, A. G. Gas-Phase Hydrogen/Deuterium Exchange of Positively Charged Mononucleotides by Use of Fourier-Transform Ion Cyclotron Resonance Mass Spectrometry. *J. Am. Soc. Mass Spectrom.* **2001**, *12*, 268–277.
23. Reed, D.; Kass, S. Hydrogen-Deuterium Exchange at Nonlabile Sites: A New Reaction Facet with Broad Implications for Structural and Dynamic Determinations. *J. Am. Soc. Mass Spectrom.* **2001**, *12*, 1163–1168.
24. Jurchen, J. C.; Cooper, R. E.; Williams, E. R. The Role of Acidic Residues and of Sodium Ion Adduction on the Gas-Phase H/D Exchange of Peptides and Peptide Dimers. *J. Am. Soc. Mass Spectrom.* **2003**, *14*, 1477–1487.
25. Crestoni, M. E.; Fornarini, S. Gas-Phase Hydrogen/Deuterium Exchange of Adenine Nucleotides. *J. Mass Spectrom.* **2003**, *38*, 854–861.
26. Cox, H. A.; Julian, R. R.; Lee, S. W.; Beauchamp, J. L. Gas-Phase H/D Exchange of Sodiated Glycine Oligomers with ND_3: Exchange Kinetics Do Not Reflect Parent Ion Structures. *J Am. Chem. Soc.* **2004**, *126*, 6485–6490.
27. Roïzman, M.; Bertoïsa, B.; Klasinc, L.; Srzic, D. Gas Phase H/D Exchange of Sodiated Amino Acids: Why Do We See Zwitterions? *J. Am. Soc. Mass Spectrom.* **2006**, *17*, 29–36.
28. Grabowski, J. J.; DePuy, C. H.; Van Doren, J. M.; Bierbaum, V. M. Gas-Phase Hydrogen-Deuterium Exchange Reactions of Anions: Kinetics and Detailed Mechanism. *J. Am. Chem. Soc.* **1985**, *107*, 7384–7389.
29. Valentine, S. J.; Clemmer, D. E. H/D Exchange Levels of Shape-Resolved Cytochrome *c* Conformers in the Gas Phase. *J. Am. Chem. Soc.* **1997**, *119*, 3558–3566.
30. Kato, S.; DePuy, C. H.; Gronert, S.; Bierbaum, V. M. Gas-Phase Hydrogen/Deuterium Exchange Reactions of Fluorophenyl Anions. *J. Am. Soc. Mass Spectrom.* **1999**, *10*, 840–847.
31. Ausloos, P.; Lias, S. G. Thermoneutral Isotope Exchange Reactions of Cations in the Gas Phase. *J. Am. Chem. Soc.* **1981**, *103*, 3641–3647.
32. Ranasinghe, A.; Cooks, R. G.; Sethi, S. K. Selective Isotopic Exchange of Polyfunctional Ions in Tandem Mass Spectrometry: Methodology, Applications, and Mechanism. *Org. Mass Spectrom.* **1992**, *27*, 77.
33. Gidden, J.; Bowers, M. T. Gas-Phase Conformations of Deprotonated and Protonated Mononucleotides Determined by Ion Mobility and Theoretical Modeling. *J. Phys. Chem.* **2003**, *107*, 12829–12837.
34. Dearden,, D. V. KINFIT: Kinetics Fitting for Coupled Ordinary Differential Equations, version 2.0 http://chemwww.byu.edu/people/dvdearden/kinfit.htm (posted April 2003).
35. Frisch, M. J.; Trucks, G. W.; Schlegel, H. B.; Scuseria,G. E.; Robb, M. A.; Cheeseman, J. R.; Montgomery, J. A., Jr.; Vreven, T.; Kudin, K. N.; Burant, J. C.; Millam, J. M.; Iyengar, S. S.; Tomasi, J.; Barone,V.; Mennucci, B.; Cossi, M.; Scalmani, G.; Rega, N.; Petersson, G. A.; Nakatsuji, H.; Hada, M.; Ehara, M.; Toyota, K.; Fukuda, R.; Hasegawa, J.; Ishida, M.; Nakajima, T.; Honda, Y.; Kitao, O.; Nakai, H.; Klene, M.; Li, X.; Knox, J. E.; Hratchian, H. P.; Cross, J. B.; Adamo, C.; Jaramillo, J.; Gomperts, R.; Stratmann, R. E.; Yazyev, O.; Austin, A. J.; Cammi, R.; Pomelli, C.; Ochterski, J. W.; Ayala, P. Y.; Morokuma, K.; Voth, G. A.; Salvador, P.; Dannenberg, J. J.; Zakrzewski, V. G.; Dapprich, S.; Daniels, A. D.; Strain, M. C.; Farkas, O.; Malick, D. K.; Rabuck, A. D.; Raghavachari, K.; Foresman, J. B.; Ortiz, J. V.; Cui, Q. A.; Baboul, G.; Clifford, S.; Cioslowski, J.; Stefanov, B. B.; Liu,G.; Liashenko, A.; Piskorz, P.; Komaromi, I.; Martin, R. L.; Fox, D. J.; Keith, T.; Al-Laham, M. A.; Peng, C. Y.; Nanayakkara, A.; Challacombe, M.;. Gill, P. M. W.; Johnson, B.; Chen, W.; Wong, M. W.; Gonzalez, C.; Pople, J. A. *Gaussian* 03, revision C. 02; Gaussian, Inc.: Wallingford, CT, 2004.
36. Allinger, N. L.; Yuh, Y. H.; Lii, J.-H. Molecular Mechanics. The MM3 Force Field for Hydrocarbons. *J. Am. Chem. Soc.* **1989**, *111*, 8551–8566.
37. Dewar, J. S.; Zoebisch, E. G.; Healy, E. F.; Stewart, J. P. AM. 1: A New General Purpose Quantum Mechanical Molecular Model. *J. Am. Chem. Soc.* **1985**, *107*, 3902–3909.
38. Foresman, J. B.; Frisch, M. J. Exploring Chemistry with Electronic Structure Methods; Gaussian, Inc.: Pittsburgh, PA, 1996.
39. Pople, J. A.; Krishnan,R.; Schlegel, H. B.; DeFrees, D.; Binkley, J. S.; Frisch, M. J.; Whiteside, R. F.; Hout, R. F.; Hehre, W. J. *Int. J. Quantum. Chem. Symp.* **1981**, 15269.
40. Liu, D.; Wyttenbach, T.; Bowers, M. T. Hydration of Mononucleotides. *J. Am. Chem. Soc.* **2006**, *128*, 15155–15163.
41. McLucky, S. A.; Glish, G. L.; Asano, K. G.; Bartmess, J. E. Protonated Water and Protonated Methanol Cluster Decompositions in a Quadrupole Ion Trap. *Int. J. Mass Spectrom.* **1991**, *109*, 171–186.
42. Gronert, S. Estimation of Effective Ion Temperatures in a Quadrupole Ion Trap. *J. Am. Soc. Mass Spectrom.* **1998**, *9*, 845–848.
43. Wyttenbach, T.; Bowers, M. T. Gas-Phase Conformations: The Ion Mobility/Ion Chromatography Method. *Top. Curr. Chem.* **2003**, *225*, 207–232.
44. Nir, E.; Imhoff, P.; Kleinermanns, K.; de Vries, M. S. REMPI Spectra of Laser Desorbed Guanosines. *J. Am. Chem. Soc.* **2000**, *122*, 8091–8092.
45. Habibi-Goudarzi, S.; McLuckey, S. Ion Trap Collisional Activation of the Deprotonated Deoxymononucleoside and Deoxydinucleoside Monophosphates. *J. Am. Soc. Mass Spectrom.* **1995**, *6*, 102–113.
46. Yang, X.; Wang, X.; Vorpagel, E. R.; Wang, L. Direct Experimental Observation of the Low Ionization Potentials of Guanine in Free Oligonucleotides by Using Photoelectron Spectroscopy. *Proc. Natl. Acad. Sci. U.S.A.* **2004**, *101*, 17588–17592.
47. Englander, S. W. Hydrogen Exchange and Mass Spectrometry: A Historical Perspective. *J. Am. Soc. Mass Spectrom.* **2006**, *17*, 1481–1489.
48. Salter, E. A.; Wierzbicki, A.; Sperl, G. Thompson, W. J. Quantum Mechanical Study of the Syn and Anti-Conformations of Solvated Cyclic GMP. *Struct. Chem.* **2003**, *14*, 527–533.
49. Kirschner, K. N.; Shields, G. C. Quantum Mechanical Investigation of Cyclic 3′,5′-Adenosine Monophosphate, the Second Hormonal Messenger. *J. Mol. Struct. (Theochem.)* **1996**, *362*, 297–304.
50. Huang, Y.; Kenttamaa, H. Theoretical Estimations of the 298 K Gas-Phase Acidities of the Purine-Based Nucleobases Adenine and Guanine. *J. Phys. Chem. A* **2004**, *108*, 4485–4490.
51. Rejnek, J.; Hanus, M.; Kabeláč, M.; Ryjáček, F.; Hobza, P. Correlated ab Initio Study of Nucleic Acid Bases and Their Tautomers in the Gas Phase, in a Microhydrated Environment, and in Aqueous Solution. Part 4. *Uracil and Thymine P. Phys. Chem., Chem. Phys.* **2005**, *7*, 2006–2017.
52. Close, D., Hernández, C., Gorb, L., Leszczynski, Influence of Microhydration on the Ionization Energy Thresholds of Thymine: Comparisons of Theoretical and Experimental Values. *J. Phys. Chem. A* **2006**, Published on Web 5/19/2006.
53. Leszczynski, J. Tautomeric Properties of Nucleic Acid Bases: Ab Initio Study. In *Encyclopedia of Computational Chemistry*; J. Wiley: New York, 1998.